International Journal of Research Publication and Reviews, Vol 4, no 12, pp 1940-1955 December 2023

International Journal of Research Publication and Reviews

Journal homepage: www.ijrpr.com ISSN 2582-7421

Fractional Order Model of Elctromagneto hydrodynamic Fluid Flow and Heat Transfer of Non-Newtonian Nanofluids

Usamatu Usman[1], Mohammed Abdulhameed[2]

[1]Department of Mathematical Science, Faculty of Science, Abubakar Tafawa Balewa University, Bauchi
[2]Department of Mathematics and Statistics, Federal Polytechnic, Bauchi

Abstract

This research work, aimed at examining the effect of fractional order, heat transfer and chemical reaction on electro-magneto-hydrodynamic flow of blood through a porous medium vessel with an externally applied magnetic field for drug delivery applications. We modeled the electro-magneto-hydrodynamic blood flow for momentum, temperature distribution and concentration with the Atangana-Baleanu fractional order derivatives and obtained the non-dimensional form of the modeled equations. Exact solution of the fractional order model equations were obtained using Laplace transform and finite Hankel transform and their inverses technique. With the aid of Mathcad software, the results were simulated and presented graphically. The results show that, as the fractional order parameter increases, both the blood velocity as well as the velocity of nanoparticles decreases, this is as a result of presence of drug forces on the nanoparticles suspended in the blood. Also, increasing Joule heating and Eckert number lead to increase in temperature distribution in the affected tumor cells within small period of time which prevent high thermal radiation exposure from killing the healthy cells within the region.

Keywords: Electromagnetohydrodynamic, Blood, Magnetic nanoparticles, Thermal radiation, Drug delivery

1.0 Introduction

A biomagnetic fluid is a type of fluid that is found in living organism or creature and reacts in presence of magnetic field. Blood can be regarded as biomagnetic fluid, in which red blood cells are magnetic in nature. Magnetic fluid dynamics is comparatively new area in fluid dynamics that study the dynamics of biomagnetic fluid in the presence of magnetic field (Esfahani et al. 2019). It is well known that blood behaves differently when flowing in large vessels in which Newtonian behavior is expected and in medium and small vessels where non-Newtonian effect appear. Human body experiences magnetic field of moderate to high intensity in many situation of day to day life. In recent times, many medical diagnostic devices especially those used in diagnosing cardiovascular disease make use of magnetic fields (Gaurav et al 2010). It is known from the magnetohydrodynamics that when a stationary transverse magnetic field is applied externally to a moving electrically conducting fluid, electrical current are induced in the fluid. The interaction between these induced current and the applied magnetic field produces a body forces (known as Lorentz force) which tends to retardate the movement of the blood (Gaurav et al 2010). The current trend for MHD flow is toward a strong magnetic field, so that the influence by electromagnetic force is noticeable. When the applied magnetic field strength is large and the conductivity fluid is an ionized gas where the density is low, the conductivity normal to the magnetic field is reduced to the spiraling of electrons and ions about the magnetic lines of force before collisions takes place and a current is induced in a direction normal to both the electric and magnetic fields. Farhad et al (2017) investigated the effect of vertical magnetic field in a two-phase blood flow (plasma and red blood cells) in a horizontal cylinder with Caputo fractional model. They assumed the blood as a non-Newtonian fluid and flow movement was as a result of an oscillating pressure gradient, the results show that the casson fluid parameter and Grashof number had a direct effect on velocity profile, while the magnetic field and Prandtl number showed the inverse effect. Tripathi and Sharma (2016) investigated the effect of magnetic field on blood flow through stenosis, inclined porous artery with a heat source using homotopy perturbation technique. They assumed that the viscosity is related to the percentage of red blood cells in the blood. The results showed that the velocity and decrease with increasing the value of magnetic field parameter, hematocritic and heat source and decreasing the Grashof number and porosity parameter. Larimi et al (2014) studied the effect of magnetic field on blood flow along a bifurcation using ferrohydrodynamics principle induced by a current wire. The found out that with increasing magnetic intensity, the wall shear stress increased significantly near the wire. They then use safe magnetic field to investigate the targeted drug delivery.

The fractional derivatives play an important in many fields such as bioengineering, mechanics, physics, the mathematical model of fractal theory, electromagnetic theory and in an electrical circuits design. Paris and George (2014) study integer and fractional order viscoelastic models in a one-dimensional blood flow solver. Their results confirm that the effect of fractional order models on hemodynamics is primarily controlled by the fractional parameter, which affect the pressure wave propagation by introducing viscoelastic dissipation in the system. Nehad and Khan (2016) present a Caputo-Fabrizio fractional derivative approach to thermal analysis of second grade fluid over an infinite oscillating vertical flat plate. Closed form solution of the fluid velocity and temperature are obtained by means of the Laplace transform method. A comparison for time derivative of integer order versus fractional order is shown graphically. It is found that fractional fluids have highest velocities. Nehad et al. (2016) present the effect of fractionalorder magnetohydrodynamic blood flow through a circular cylinder in the Caputo type.

To date, numerous mathematical model have been develop to investigate the exhibited behavior of fractional order model of fluid flow. Keeping in mind the above studies, in the present work we will develop a mathematical model concerning fractional order derivatives on fluid flow and heat transfer of non-Newtonian nano-fluids. The non-Newtonian biviscosity fluid model with the influence of the body acceleration, applied magnetic field, applied electric field, thermal radiation, soret effect and chemical reaction will be incorporated into the model of blood flow through a porous circular vessels for drug delivery application.

2.0 Mathematical model

In the present work, we consider the non-Newtonian biviscosity fluid with magnetic nano particles flowing through a straight tube with constant radius and assume that the magnetic nanoparticles are distributed equally into the blood stream. The motion of the magnetic nanoparticles is controlled by the magnetic field created from outside of the body. The equation of nanoparticles is governed by Newton's second law of motion (Maiti et al (2021)).the momentum equation, the energy equation and the concentration equation based on the above assumption is taken as presented by Maiti et al (2021).

2.1 Applied Magnetic field

Since the blood is an electrically conducting in the presence of magnetic field. Therefore, the generalized Ohm's law is given (Ellahi (2010), and Akbarzadeh (2016)):

By Ohm's law, the current density J is expressed by

$$J = \sigma_e \left(E + V \times B \right) \quad \dots (1)$$

where E is the electrical field intensity, σ_e is the electrical conductivity, B is the magnetic flux intensity and V is the velocity vector.

The volumetric heat generation due to joule heating effect and electromagnetic interaction is defined by:

$$\frac{\vec{J}.\vec{J}}{\sigma_e} \quad \dots (2)$$

$$V \times \mathrm{B} = \begin{bmatrix} i & j & k \\ 0 & u & 0 \\ B_0 & 0 & 0 \end{bmatrix} = -B_0 \bar{u}(\bar{r}, \bar{t}) k \quad \dots (3)$$

$$\vec{J}.\vec{J} = \sigma_e^{\,2} \ (E^{\,2} + B_0^{\,2} \overline{u^2}) \quad \dots (4)$$

By substituting equation (4) into (2) we obtain:

$$\frac{\vec{J}.\vec{J}}{\sigma_e} = \sigma_e (E^{\,2} + B_0^{\,2} u^2). \quad \dots (5)$$

where $u(r,t)$ is the axial velocity of the blood flow.

2.2 Electrostatic potential field

According to the theory of electrostatics, the net charge density ρ_e is given by the Poisson equation (Escandon et al 2015).

$$\frac{\partial^2 \Phi}{\partial \ x^2} + \frac{\partial^2 \Phi}{\partial \ r^2} = -\frac{\rho_e}{\in} \quad \dots (6)$$

Where Φ, is the total electric potential within the channel and $\in$ denotes the dielectric permittivity of the fluid. The charge distribution is determined from the potential at the wall, ζ, called zeta potential. The total electric potential, Φ, is given by

$$\Phi = \varphi + \psi \quad \ldots (7)$$

Where φ is the externally applied electric potential, and ψ is the electric potential due to double layer at equilibrium state.

$\varphi = \varphi_0 + xE_x$ and φ_0 is the value of the imposed potential at $x = 0$. The E_x field is independent of the position and is assumed constant in the longitudinal direction, therefore taking the above assumption into consideration equation (6) becomes

$$\frac{d^2\psi}{d\bar{r}^2} = -\frac{\rho_e}{\in} \quad \ldots (8)$$

Where the net charge density for electrolyte solution is given by the Boltzman distribution

$$\rho_e = -2z\eta_0 e \sinh\left(\frac{ze\Psi}{k_B T}\right) \quad \ldots (9)$$

where z, $\eta_{0,}, e, k_B$ and T are the valence , ion density, fundamental charge, Boltzmann constant and absolute temperature, respectively. Equation (8) subject to the following boundary conditions at the top and bottom of the walls of the artery, are

$$\psi = \varsigma_1 \quad \text{at } \bar{r} = 0, \quad \ldots (10)$$

$$\psi = \varsigma_2 \quad \text{at } \bar{r} = 1 \quad \ldots (11)$$

The wall potential are axially invariant, therefore, in order to simplify the analysis, we use the Debye-Hückel approximation, that is,

$\sinh\left(\frac{ze\Psi}{k_B T}\right) \approx \left(\frac{ze\Psi}{k_B T}\right)$ for $\left(\frac{ze\Psi}{k_B T}\right)$ << 1, hence equation (8) becomes

$$\frac{d^2\psi}{d\ y^2} = k_e^2\ \psi \quad \ldots (12)$$

Where, $k_e^2 = \left(\frac{2\eta_0 z^2 e^2}{\in k_B T}\right)$ is the Debye-Hückel parameter.

The solution of equation (12) subject to the boundary conditions (10) and (11) is given by

$$\psi = \varsigma_1 \left\{ \left[\frac{\frac{\varsigma_2}{\varsigma_1} - e^{-2kH}}{2\sinh[2kH]} \right] e^{k\bar{r}} + \left[1 - \frac{\frac{\varsigma_2}{\varsigma_1} - e^{-2kH}}{2\sinh[2kH]} \right] e^{-k\bar{r}} \right\} \quad \ldots (13)$$

From equation (8) and (12) we have that

$$\rho_e = -k_e{}^2 \psi \in \quad \ldots (14)$$

Substituting equation (8) into (9) we have

$$\rho_e = -k_e{}^2 \in \varsigma_1 \left\{ \left[\frac{\frac{\varsigma_2}{\varsigma_1} - e^{-2kH}}{2\sinh[2kH]} \right] e^{k\bar{r}} + \left[1 - \frac{\frac{\varsigma_2}{\varsigma_1} - e^{-2kH}}{2\sinh[2kH]} \right] e^{-k\bar{r}} \right\} \quad \ldots (15)$$

Putting $R_{\varsigma} = \frac{\varsigma_2}{\varsigma_1}$, $A = \left[\frac{\frac{\varsigma_2}{\varsigma_1} - e^{-2kH}}{2\sinh[2kH]} \right]$, $B = (1 - A)$ we see that equation (15) becomes

$$\rho_e = -k_e^2 \in \varsigma_1 \left(Ae^{k\bar{r}} + Be^{-k\bar{r}} \right) \quad \ldots (16)$$

Multiplying equation (16) by E we get

$$\rho_e E = -E \in k^2 \varsigma_1 \left(Ae^{k\bar{r}} + Be^{-k\bar{r}} \right). \quad \ldots (17)$$

2.3 Basic Flow Equations

The momentum equation is taken as

$$\frac{\partial \bar{u}}{\partial \bar{t}} = \frac{1}{\rho}\frac{\partial \bar{p}}{\partial \bar{z}} + \nu\left(1 + \frac{1}{\beta}\right)\left[\frac{\partial^2 \bar{u}}{\partial \bar{r}^2} + \frac{1}{\bar{r}}\frac{\partial \bar{u}}{\partial \bar{r}}\right] + \frac{KN}{\rho}(\bar{v} - \bar{u}) + \frac{G(\bar{t})}{\rho} - \frac{\mu}{\rho k_p}\bar{u} - \frac{\sigma B_0^2}{\rho}\bar{u}$$
$$+ g\beta_T(\overline{T} - \overline{T_w}) + g\beta_C(\overline{C} - \overline{C_w}) + \rho_e E \quad \ldots (18)$$

The equation of nanoparticles when the particles experience only fluidic force is given by

$$m\frac{\partial \bar{v}}{\partial \bar{t}} = K_s\left(\bar{u} - \bar{v}\right) \quad \ldots (19)$$

Where all the variables are functions of r and t, the variables $\bar{u}$, $\bar{v}$, $\overline{T}$ and $\overline{C}$ denotes the blood velocity, particle velocity, temperature and concentration respectively, m is the mass of the nanoparticle, k_p the permeability of the porous medium, β is the viscosity parameter, N the number of magnetic particle per unit volume, B_0 is the magnetic field strength $\frac{KN}{\rho}(\bar{v} - \bar{u})$ is the force between magnetic particles and fluidic due to their relative motion, g, β_T and β_C are the gravity, coefficient of thermal expansion and concentration expansion respectively, $\overline{T_w}$ is the temperature at the vessel wall, $\overline{C_w}$ denotes the mass concentration at the vessel wall, ρ is the fluid density, $\frac{\partial}{\partial t}$ is the material time derivative, ρ_e denote the net charge density of the applied electric field in the blood flow and E is the external electric field imposed at the ends of the arterial wall.

The periodic body acceleration, $G(\bar{t})$, is defined as

$$G(\bar{t}) = \overline{A_0}\cos\left(\bar{k}\bar{t} + \phi_0\right) \quad \ldots (20)$$

Where, $\overline{A_0}$ is the amplitude, ϕ_0 gives the difference with the pressure gradient, $\bar{k}$ denotes the frequency of the body acceleration.

The energy equation is taken as

$$\rho c_p \frac{\partial \overline{T}}{\partial \bar{t}} = k\left[\frac{\partial^2 \overline{T}}{\partial \bar{r}^2} + \frac{1}{\bar{r}}\frac{\partial \overline{T}}{\partial \bar{r}}\right] - \frac{\partial \bar{q}_r}{\partial \bar{r}} + \overline{Q_m} + \frac{J.J}{\sigma_e} \quad \ldots (21)$$

where ρ is the fluid density, C_P is the specific heat capacity of the fluid, $\overline{Q_m}$ is the metabolic heat source coefficient, $\vec{J}$ is the current density given by the Ohm's law, σ_e is the electrical conductivity, k is the thermal conductivity of the fluid, $\frac{\vec{j}\,\vec{j}}{\sigma_e}$, is the Joule heating effect created by the current density. The approximated heat flux is given by

$$-\frac{\partial \overline{q}_r}{\partial \overline{r}} = 4\alpha_2{}^2\left(\overline{T} - T_\infty\right) \qquad \dots (22)$$

Where $\alpha_2{}^2 = \int_0^\infty \beta\chi \frac{\partial B}{\partial T}$, and β denotes the absorption coefficient of radiation, χ be the frequency, B the Planck's constant, T_∞ is the ambient temperature.

The thermo-diffusion equation is given as

$$\frac{\partial \overline{C}}{\partial \overline{t}} = D_m\left[\frac{\partial^2 \overline{C}}{\partial \overline{r}^2} + \frac{1}{\overline{r}}\frac{\partial \overline{C}}{\partial \overline{r}}\right] + \frac{D_m K_T}{T_\infty}\left[\frac{\partial^2 \overline{T}}{\partial \overline{r}^2} + \frac{1}{\overline{r}}\frac{\partial \overline{T}}{\partial \overline{r}}\right] - k_0\left(\overline{C} - Cw\right) \qquad \dots (23)$$

Where D_m, K_T, and k_0 are the mass diffusivity of blood, thermal diffusion ratio and chemical reaction coefficient respectively, the term $\frac{D_m K_T}{T_\infty}\left[\frac{\partial^2 \overline{T}}{\partial \overline{r}^2} + \frac{1}{\overline{r}}\frac{\partial \overline{T}}{\partial \overline{r}}\right]$ represent the soret effect and the term $\frac{D_m K_T}{T_\infty}\left[\frac{\partial^2 \overline{T}}{\partial \overline{r}^2} + \frac{1}{\overline{r}}\frac{\partial \overline{T}}{\partial \overline{r}}\right]$ defines the chemical reaction effect.

We consider the following set of boundary conditions

$$\begin{aligned}
&\overline{u}(R_0, t) = 0, \overline{v}(R_0, t) = 0,\\
&\overline{T}(R_0, t) = T_{w,} \overline{C}(R_0, t) = C_w\\
&\frac{\partial \overline{u}(0,t)}{\partial \overline{r}} = 0, \frac{\partial \overline{T}(0,t)}{\partial \overline{r}} = 0, \frac{\partial \overline{C}}{\partial \overline{r}} = 0
\end{aligned} \qquad \dots (24)$$

Let us consider the following non-dimensional parameters

$$r = \frac{\overline{r}}{R_0},\ t = \frac{u_0 \overline{t}}{R_0},\ u = \frac{\overline{u}}{u_0},\ v = \frac{\overline{v}}{u_0},\ p = \frac{\overline{p}}{\rho u_0^2}, z = \frac{\overline{z}}{R_0},\ \omega = \frac{R_0 \overline{\omega}}{u_0},\ k = \frac{\overline{r} R_0}{u_0},\ l = \overline{l} R_0,\ A_0 = \frac{R_0 \overline{A_0}}{u_0^2},$$

$$\theta = \frac{\overline{T} - T_w}{T_w - T_\infty},\ Q_m = \frac{R_0 \overline{Q_m}}{u_0 \rho c_p (T_w - T_\infty)},\ \phi = \frac{\overline{C} - C_w}{C_w - C_\infty}, \qquad \dots (25)$$

By the use of non-dimensional variables (25), equations (18), (19), (21) and (23) becomes

$$\frac{\partial u}{\partial t} = -\frac{\partial p}{\partial z} + \frac{1}{\mathrm{Re}}\left(1 + \frac{1}{\beta}\right)\left[\frac{\partial^2 u}{\partial r^2} + \frac{1}{r}\frac{\partial u}{\partial r}\right] + \frac{P_c}{\mathrm{Re}}(v - u) + A_0\cos(kt + \phi_0)$$

$$+\frac{1}{Da\,\mathrm{Re}}u + \frac{Ha^2}{\mathrm{Re}}u + \frac{Gr}{\mathrm{Re}^2}\theta + \frac{Gc}{\mathrm{Re}^2}\phi + l^2\left(Ae^{lr} + Be^{-lr}\right) \qquad \dots (26)$$

$$P_m\frac{\partial v}{\partial t} = u - v \qquad \dots (27)$$

$$\frac{u_0\rho c_p(T_w-T_\infty)}{R_0}\frac{\partial\theta}{\partial t}=\frac{k(T_w-T_\infty)}{R_0^2}\left[\frac{\partial^2\theta}{\partial r^2}+\frac{1}{r}\frac{\partial\theta}{\partial r}\right]-4\alpha_2^2(T_w-T_\infty)\theta$$
$$+\frac{Q_m u_0\rho c_p(T_w-T_\infty)}{R_0}+\sigma_e\left(E^2+B_0^2u_0^2u^2\right) \quad \text{… (28)}$$

$$\mathrm{Re}\,Sc\frac{\partial\phi}{\partial t}=\left[\frac{\partial^2\phi}{\partial r^2}+\frac{1}{r}\frac{\partial\phi}{\partial r}\right]+SrSc\left[\frac{\partial^2\theta}{\partial r^2}+\frac{1}{r}\frac{\partial\theta}{\partial r}\right]-K_cS_c\,\mathrm{Re}^2\,\phi \quad \text{… (29)}$$

Where $\mathrm{Re}=\frac{R_0u_0}{\upsilon}$ the Reynolds number, $Ha=B_0R_0\sqrt{\frac{\sigma}{\rho\upsilon}}$ the Hartmann number, $Da=\frac{k_p}{R_0^2}$ the Darcy parameter, $P_c=\frac{KNR_0^2}{\mu}$ the particle concentration parameter, $Gr=\frac{gB_T(T_w-T_\infty)R_0^3}{\upsilon^2}$ the thermal Grash of number, $Gc=\frac{gB_C(C_w-C_\infty)R_0^3}{\upsilon^2}$ the mass Grash of number, $P_m=\frac{mu_0}{KR_0}$ the particle mass parameter. $\mathrm{Pr}=\frac{\mu c_p}{k}$ the Prandtl number, $Pe=\mathrm{Re}\cdot\mathrm{Pr}$ the Peclet number, $R=\frac{4\alpha_2^2R_0^2}{k}$ the thermal radiation parameter, the chemical reaction parameter, $E_c=\frac{\mu u^2}{k(T_w-T_\infty)}$ the Eckert number and $\lambda=\frac{\sigma_eR_0^2E^2}{k(T_w-T_\infty)}$ the Joule heating parameter respectively.

Grashof number, $P_m=\frac{mu_0}{KR_0}$ the particle mass parameter $Sc=\frac{\nu}{D_m}$ the Schmidt number, $Sr=\frac{D_mK(T_w-T_\infty)\mu c_p}{\nu T_\infty(C_w-C_\infty)}$ the Soret number, $K_c=\frac{K\nu}{u_0^2}$.

In non-dimensional form, the boundary conditions become

$$u(1,t)=0, v(1,t)=0,$$
$$\theta(1,t)=0, \phi(1,t)=0$$
$$\frac{\partial u(0,t)}{\partial r}=0, \frac{\partial\theta(0,t)}{\partial r}=0, \frac{\partial\phi}{\partial r}=0 \quad \text{… (30)}$$

Now, replacing the time classical derivatives with the Atangana-Baleanu time fractional order derivatives defined by

$$D_t^\alpha f(t)=\frac{B(\alpha)}{1-\alpha}\int_0^t f'(\tau)E_\alpha\left[-\frac{\alpha(t-\tau)}{1-\alpha}\right]d\tau \quad \text{… (31)}$$

Where $0<\alpha<1$, α is known as the fractional order parameter. The equations (26)-(29) takes the form

$$D_t^\alpha u=(b_0+b_1\cos(\omega t))+\frac{1}{\mathrm{Re}}\left(1+\frac{1}{\beta}\right)\left[\frac{\partial^2u}{\partial r^2}+\frac{1}{r}\frac{\partial u}{\partial r}\right]+\frac{P_c}{\mathrm{Re}}(v-u)+A_0\cos(kt+\phi_0)$$
$$+\frac{1}{Da\,\mathrm{Re}}u+\frac{Ha^2}{\mathrm{Re}}u+\frac{Gr}{\mathrm{Re}^2}\theta+\frac{Gc}{\mathrm{Re}^2}\phi+l^2\left(Ae^{lr}+Be^{-lr}\right) \quad \text{… (32)}$$

$$P_mD_t^\alpha v=u-v \quad \text{… (33)}$$

$$PeD_t^{\alpha}\theta = \left[\frac{\partial^2\theta}{\partial r^2} + \frac{1}{r}\frac{\partial\theta}{\partial r}\right] + R\theta + PeQ_m + Ha^2E_c + \lambda \quad \dots (34)$$

$$\operatorname{Re} ScD_t^{\alpha}\phi = \left[\frac{\partial^2\phi}{\partial r^2} + \frac{1}{r}\frac{\partial\phi}{\partial r}\right] + SrSc\left[\frac{\partial^2\theta}{\partial r^2} + \frac{1}{r}\frac{\partial\theta}{\partial r}\right] - K_cS_c\operatorname{Re}^2\phi \quad \dots (35)$$

3.0 Analytical solution

Taking the Laplace transform of equations (32)-(35) subject to the initial conditions we have

$$\frac{s^{\alpha}u(r,s)}{s^{\alpha}(1-\alpha)+\alpha} = \left(\frac{b_0}{s} + \frac{b_1}{s^2+\omega^2}\right) + \frac{1}{\operatorname{Re}}\left(1+\frac{1}{\beta}\right)\left[\frac{\partial^2 u}{\partial r^2} + \frac{1}{r}\frac{\partial u}{\partial r}\right] + \frac{P_c}{\operatorname{Re}}(v-u) + A_0\left(\frac{s\cos\phi_0 - k\sin\phi_0}{k^2+s^2}\right)$$
$$+\frac{1}{Da\operatorname{Re}}u + \frac{Ha^2}{\operatorname{Re}}u + \frac{Gr}{\operatorname{Re}^2}\theta + \frac{Gc}{\operatorname{Re}^2}\phi + l^2\left(Ae^{lr} + Be^{-lr}\right) \quad \dots (36)$$

$$\frac{P_m s^{\alpha}v(r,s)}{s^{\alpha}(1-\alpha)+\alpha} = u - v \quad \dots (37)$$

$$\frac{Pes^{\alpha}\theta(r,s)}{s^{\alpha}(1-\alpha)+\alpha} = \left[\frac{\partial^2\theta}{\partial r^2} + \frac{1}{r}\frac{\partial\theta}{\partial r}\right] + R\theta + \frac{PeQ_m}{s} + \frac{Ha^2E_c}{s} + \frac{\lambda}{s} \quad \dots (38)$$

$$\frac{\operatorname{Re} Scs^{\alpha}\phi(r,s)}{s^{\alpha}(1-\alpha)+\alpha} = \left[\frac{\partial^2\phi}{\partial r^2} + \frac{1}{r}\frac{\partial\phi}{\partial r}\right] + SrSc\left[\frac{\partial^2\theta}{\partial r^2} + \frac{1}{r}\frac{\partial\theta}{\partial r}\right] - K_cS_c\operatorname{Re}^2\phi \quad \dots (39)$$

Where u, v, θ, and ϕ are functions of r and s with $s > 0$ as the Laplace parameter.

The set of boundary values to the variables yield

$$u(1,s) = 0, v(1,s) = 0,$$
$$\theta(1,s) = 0, \phi(1,s) = 0$$
$$\frac{\partial u(0,s)}{\partial r} = 0, \frac{\partial\theta(0,s)}{\partial r} = 0, \frac{\partial\phi(0,s)}{\partial r} = 0 \quad \dots (40)$$

We now take the finite the zeroth order Hankel transform of equations (36)-(39) defined by

$$\mathrm{H}_0\{f(r)\} = \int_0^1 f(r)rJ_0(r_n,r)dr \quad \dots (41)$$

And $\mathrm{H}_0\{u(r,s)\}$ is denoted as $u_H(r_n,s)$, $\mathrm{H}_0\{const\}$ is denoted as $const\cdot\frac{J_1(r_n)}{r_n}$, and $\mathrm{H}_0\left\{\frac{\partial^2 u}{\partial r^2} + \frac{1}{r}\frac{\partial u}{\partial r}\right\}$ is denoted as $-r_n^2\cdot u_H(r_n,s)$.

The equations take the form

$$u_H(r_n,s)=\frac{C_0(s^\alpha+B_1)(s^\alpha+B_2)}{(s^\alpha+B_{1n})(s^\alpha+B_{2n})}\left[\left\{\begin{array}{l}\frac{b_0}{s}+\frac{b_1}{s^2+\omega^2}+A_0\left(\frac{s\cos\phi_0-k\sin\phi_0}{k^2+s^2}\right)+\frac{GrC_3}{\mathrm{Re}^2A_{2n}s}\left(\frac{s^\alpha+C_4}{s^\alpha+A_{5n}}\right)\\-\frac{GcSrScC_0C_3r_n^2(s^\alpha+C_1)(s^\alpha+C_4)}{\mathrm{Re}^2A_{2n}A_{4n}s(s^\alpha+A_{6n})(s^\alpha+A_{5n})}\end{array}\right\}\cdot\frac{J_1(r_n)}{r_n}\\+\frac{l^2(B-A)}{(l^2+r^2)^{\frac{3}{2}}}\right]$$

… (42)

$$v_H(r_n,s)=\frac{C_0C_5(s^\alpha+C_1)(s^\alpha+B_1)(s^\alpha+B_2)}{(s^\alpha+C_6)(s^\alpha+B_{1n})(s^\alpha+B_{2n})}\left[\left\{\begin{array}{l}\frac{b_0}{s}+\frac{b_1}{s^2+\omega^2}+A_0\left(\frac{s\cos\phi_0-k\sin\phi_0}{k^2+s^2}\right)\\+\frac{GrC_3}{\mathrm{Re}^2A_{2n}s}\left(\frac{s^\alpha+C_4}{s^\alpha+A_{5n}}\right)-\frac{GcSrScC_0C_3r_n^2(s^\alpha+C_1)(s^\alpha+C_4)}{\mathrm{Re}^2A_{2n}A_{4n}s(s^\alpha+A_{6n})(s^\alpha+A_{5n})}\end{array}\right\}\cdot\frac{J_1(r_n)}{r_n}\\+\frac{l^2(B-A)}{(l^2+r^2)^{\frac{3}{2}}}\right]$$

… (43)

$$\theta_H(r_n,s)=\frac{C_3s^\alpha+C_2}{s(A_{2n}s^\alpha+A_{1n})}\cdot\frac{J_1(r_n)}{r_n}$$

… (44)

$$\phi_H(r_n,s)=-\frac{SrScC_0r_n^2(s^\alpha+C_1)(C_3s^\alpha+C_2)}{s(A_{4n}s^\alpha+A_{3n})(A_{2n}s^\alpha+A_{1n})}\cdot\frac{J_1(r_n)}{r_n}$$

… (45)

Where $C_0=1-\alpha$, $C_1=\frac{\alpha}{1-\alpha}$, $C_2=C_1C_2\left(PeQ_m+Ha^2E_c\right)$, $C_3=C_0\left(PeQ_m+Ha^2E_c\right)$, $A_{1n}=C_1C_0\left(r_n^2-R-\lambda\right)$, $A_{2n}=Pe+C_0\left(r_n^2-R-\lambda\right)$, $A_{3n}=C_1C_0r_n^2+C_1C_0K_c\,\mathrm{Re}$ and $A_{4n}=\mathrm{Re}\,Sc+C_0r_n^2+C_0ScK_c\,\mathrm{Re}$, $B_1=\frac{-(C_1P_m+2C_0C_1)-\sqrt{\Delta}}{2(P_m+C_0)}$, $B_2=\frac{-(C_1P_m+2C_0C_1)+\sqrt{\Delta}}{2(P_m+C_0)}$,

$\Delta=(C_1P_m+2C_0C_1)^2-4(P_m+C_0)C_0C_1^2$, $B_{1n}=\frac{-\left[C_0C_1+C_n(C_1P_m+2C_0C_1)+C_0C_1P_cP_m\right]-\sqrt{\Delta_n}}{2\left[(P_m+C_0)(1+C_n)+C_0P_cP_m\right]}$,

$B_{2n}=\frac{-\left[C_0C_1+C_n(C_1P_m+2C_0C_1)+C_0C_1P_cP_m\right]+\sqrt{\Delta_n}}{2\left[(P_m+C_0)(1+C_n)+C_0P_cP_m\right]}$, $C_n=\frac{C_0\left[Da\left(1+\frac{1}{\beta}\right)r_n^2+Ha^2+1\right]}{Da\,\mathrm{Re}}$,

$\Delta_n=\left(C_0C_1+C_n(C_1P_m+2C_0C_1)+C_0C_1P_cP_m\right)^2-4\left[(P_m+C_0)(1+C_n)+C_0P_cP_m\right]C_0C_1^2C_n$, $C_4=\frac{C_2}{C_3}$,

$A_{5n}=\frac{A_{1n}}{A_{2n}}$, $A_{6n}=\frac{A_{3n}}{A_{4n}}$.

Taking the inverse Laplace transform from equation (42) to (45) we get

$$u_H(r_n,t)=\left[F_{1n}(t)+F_{2n}(t)+F_{3n}(t)+F_{4n}(t)-F_{5n}(t)+F_{6n}(t)\right]\cdot\frac{J_1(r_n)}{r_n}$$

… (46)

$$v_H\left(r_n,t\right)=\left[F_{7n}(t)+F_{8n}(t)+F_{9n}(t)+F_{10n}(t)-F_{11n}(t)+F_{12n}(t)\right]\cdot\frac{J_1(r_n)}{r_n} \quad \ldots (47)$$

$$\theta_H\left(r_n,t\right)=F_{13n}(t)\cdot\frac{J_1(r_n)}{r_n} \quad \ldots (48)$$

$$\phi_H\left(r_n,t\right)=F_{14n}(t)\cdot\frac{J_1(r_n)}{r_n} \quad \ldots (49)$$

Where

$$F_{1n}(t)=\frac{C_0\left(B_1-B_{1n}\right)\left(B_2-B_{1n}\right)b_0}{\left(B_{2n}-B_{1n}\right)}\left[R_{\alpha,-1}(-B_{1n},t)-R_{\alpha,-1}(-B_{2n},t)\right],$$

$$F_{2n}(t)=\frac{C_0\left(B_1-B_{1n}\right)\left(B_2-B_{1n}\right)b_0}{\left(B_{2n}-B_{1n}\right)}\left[b_1\cos(\omega t)\right]\left(F_\alpha(-B_{1n},t)-F_\alpha(-B_{2n},t)\right),$$

$$F_{3n}(t)=\frac{C_0\left(B_1-B_{1n}\right)\left(B_2-B_{1n}\right)b_0}{\left(B_{2n}-B_{1n}\right)}\left[A_0\cos(kt+\phi_0)\right]\left(F_\alpha(-B_{1n},t)-F_\alpha(-B_{2n},t)\right),$$

$$F_{4n}(t)=\frac{GrC_3C_0\left(B_1-B_{1n}\right)\left(B_2-B_{1n}\right)}{\mathrm{Re}^2A_{2n}\left(B_{2n}-B_{1n}\right)}\left[\begin{array}{l}\frac{C_4-B_{1n}}{A_{5n}-B_{1n}}R_{\alpha,-1}(-B_{1n},t)-\frac{C_4-A_{5n}}{C_4-B_{1n}}R_{\alpha,-1}(-A_{5n},t)\\-\frac{C_4-A_{5n}}{A_{5n}-B_{2n}}R_{\alpha,-1}(-A_{5n},t)-\frac{C_4-B_{2n}}{A_{5n}-B_{2n}}R_{\alpha,-1}(-B_{2n},t)\end{array}\right],$$

$$F_{5n}(t)=\frac{GcSrScC_0C_3r_n^2\left(B_1-B_{1n}\right)\left(B_2-B_{1n}\right)}{\mathrm{Re}^2A_{2n}\left(B_{2n}-B_{1n}\right)\left(A_{5n}-A_{6n}\right)}\left[\begin{array}{l}\frac{\left(C_1-A_{6n}\right)\left(C_4-A_{6n}\right)}{\left(A_{6n}-B_{1n}\right)}R_{\alpha,-1}(-B_{1n},t)\\-\frac{\left(C_1-A_{6n}\right)\left(C_4-A_{6n}\right)}{\left(A_{6n}-B_{1n}\right)}R_{\alpha,-1}(-A_{6n},t)\\+\frac{\left(C_1-A_{5n}\right)\left(C_4-A_{5n}\right)}{\left(A_{5n}-B_{1n}\right)}R_{\alpha,-1}(-B_{1n},t)\\+\frac{\left(C_1-A_{5n}\right)\left(C_4-A_{5n}\right)}{\left(A_{5n}-B_{1n}\right)}R_{\alpha,-1}(-A_{5n},t)\\+\frac{\left(C_1-A_{5n}\right)\left(C_4-A_{5n}\right)}{\left(A_{5n}-B_{2n}\right)}R_{\alpha,-1}(-B_{2n},t)\\-\frac{\left(C_1-A_{5n}\right)\left(C_4-A_{5n}\right)}{\left(A_{5n}-B_{2n}\right)}R_{\alpha,-1}(-A_{5n},t)\\-\frac{\left(C_1-A_{6n}\right)\left(C_4-A_{6n}\right)}{\left(A_{6n}-B_{2n}\right)}R_{\alpha,-1}(-B_{2n},t)\\+\frac{\left(C_1-A_{6n}\right)\left(C_4-A_{6n}\right)}{\left(A_{6n}-B_{2n}\right)}R_{\alpha,-1}(-A_{6n},t)\end{array}\right],$$

$$F_{6n}(t)=\frac{C_0\left(B_1-B_{1n}\right)\left(B_2-B_{1n}\right)}{\left(B_{2n}-B_{1n}\right)}\frac{l^3\left(B-A\right)}{\left(l^2+r^2\right)^{\frac{3}{2}}}\left[F_\alpha(-B_{1n},t)-F_\alpha(-B_{2n},t)\right]$$

$$F_{7n}(t)=\frac{C_0\left(B_1-B_{1n}\right)\left(B_2-B_{1n}\right)b_0}{\left(B_{2n}-B_{1n}\right)}\begin{bmatrix}\left(\frac{C_1-B_{1n}}{C_6-B_{1n}}\right)R_{\alpha,-1}(-B_{1n},t)-\left(\frac{C_1-C_6}{C_6-B_{1n}}\right)R_{\alpha,-1}(-C_6,t)\\-\left(\frac{C_1-B_{21n}}{C_6-B_{2n}}\right)R_{\alpha,-1}(-B_{2n},t)+\left(\frac{C_1-C_6}{C_6-B_{2n}}\right)R_{\alpha,-1}(-C_6,t)\end{bmatrix},$$

$$F_{8n}(t)=\frac{C_0\left(B_1-B_{1n}\right)\left(B_2-B_{1n}\right)}{\left(B_{2n}-B_{1n}\right)}\left[b_1\cos(\omega t)\right]\begin{pmatrix}\left(\frac{C_1-B_{1n}}{C_6-B_{1n}}\right)F_\alpha(-B_{1n},t)-\left(\frac{C_1-B_{1n}}{C_6-B_{1n}}\right)F_\alpha(-C_6,t)\\-\left(\frac{C_1-B_{2n}}{C_6-B_{2n}}\right)F_\alpha(-B_{2n},t)+\left(\frac{C_1-B_{2n}}{C_6-B_{2n}}\right)F_\alpha(-C_6,t)\end{pmatrix},$$

$$F_{9n}(t)=\frac{C_0\left(B_1-B_{1n}\right)\left(B_2-B_{1n}\right)}{\left(B_{2n}-B_{1n}\right)}\left[A_0\cos(kt+\phi_0)\right]\begin{pmatrix}\left(\frac{C_1-B_{1n}}{C_6-B_{1n}}\right)F_\alpha(-B_{1n},t)-\left(\frac{C_1-B_{1n}}{C_6-B_{1n}}\right)F_\alpha(-C_6,t)\\-\left(\frac{C_1-B_{2n}}{C_6-B_{2n}}\right)F_\alpha(-B_{2n},t)+\left(\frac{C_1-B_{2n}}{C_6-B_{2n}}\right)F_\alpha(-C_6,t)\end{pmatrix},$$

$$F_{10n}(t)=\frac{GrC_3C_0\left(B_1-B_{1n}\right)\left(B_2-B_{1n}\right)}{\mathrm{Re}^2A_{2n}\left(B_{2n}-B_{1n}\right)}\begin{bmatrix}\frac{C_4-B_{1n}}{A_{5n}-B_{1n}}R_{\alpha,-1}(-B_{1n},t)-\frac{C_4-A_{5n}}{C_4-B_{1n}}R_{\alpha,-1}(-A_{5n},t)\\-\frac{C_4-A_{5n}}{A_{5n}-B_{2n}}R_{\alpha,-1}(-A_{5n},t)-\frac{C_4-B_{2n}}{A_{5n}-B_{2n}}R_{\alpha,-1}(-B_{2n},t)\end{bmatrix},$$

$$F_{11n}(t)=\frac{GcSrScC_0C_3r_n^2\left(B_1-B_{1n}\right)\left(B_2-B_{1n}\right)}{\mathrm{Re}^2A_{2n}\left(B_{2n}-B_{1n}\right)\left(A_{5n}-A_{6n}\right)}\begin{bmatrix}\frac{\left(C_1-A_{6n}\right)\left(C_4-A_{6n}\right)}{\left(A_{6n}-B_{1n}\right)}R_{\alpha,-1}(-B_{1n},t)\\-\frac{\left(C_1-A_{6n}\right)\left(C_4-A_{6n}\right)}{\left(A_{6n}-B_{1n}\right)}R_{\alpha,-1}(-A_{6n},t)\\+\frac{\left(C_1-A_{5n}\right)\left(C_4-A_{5n}\right)}{\left(A_{5n}-B_{1n}\right)}R_{\alpha,-1}(-B_{1n},t)\\+\frac{\left(C_1-A_{5n}\right)\left(C_4-A_{5n}\right)}{\left(A_{5n}-B_{1n}\right)}R_{\alpha,-1}(-A_{5n},t)\\+\frac{\left(C_1-A_{5n}\right)\left(C_4-A_{5n}\right)}{\left(A_{5n}-B_{2n}\right)}R_{\alpha,-1}(-B_{2n},t)\\-\frac{\left(C_1-A_{5n}\right)\left(C_4-A_{5n}\right)}{\left(A_{5n}-B_{2n}\right)}R_{\alpha,-1}(-A_{5n},t)\\-\frac{\left(C_1-A_{6n}\right)\left(C_4-A_{6n}\right)}{\left(A_{6n}-B_{2n}\right)}R_{\alpha,-1}(-B_{2n},t)\\+\frac{\left(C_1-A_{6n}\right)\left(C_4-A_{6n}\right)}{\left(A_{6n}-B_{2n}\right)}R_{\alpha,-1}(-A_{6n},t)\end{bmatrix},$$

$$F_{12n}(t)=\frac{C_0(B_1-B_{1n})(B_2-B_{1n})}{(B_{2n}-B_{1n})}\frac{l^3(B-A)}{(l^2+r^2)^{\frac{3}{2}}}\left[\begin{array}{l}\left(\frac{C_1-B_{1n}}{C_6-B_{1n}}\right)F_\alpha(-B_{1n},t)-\left(\frac{C_1-B_{2n}}{C_6-B_{2n}}\right)F_\alpha(-B_{2n},t)\\-\left(\frac{C_1-C_6}{C_6-B_{1n}}\right)F_\alpha(-C_6,t)+\left(\frac{C_1-C_6}{C_6-B_{2n}}\right)F_\alpha(-C_6,t)\end{array}\right],$$

$$F_{13n}(t)=\frac{C_7}{A_{2n}}\left[1+(C_4-A_{5n})F_\alpha(-A_{5n},t)\right],$$

$$F_{14n}(t)=-\frac{SrScC_0r_n^2}{(A_{6n}-A_{5n})}\left[(C_1-A_{6n})(C_4-A_{6n})R_{\alpha,-1}(-A_{6n},t)-(C_1-A_{5n})(C_4-A_{5n})R_{\alpha,-1}(-A_{5n},t)\right]$$

Taking the Hankel inverse of the equations (46)-(49) we get

$$u(r,t)=2\sum_{n=1}^{\infty}\frac{J_0(rr_n)}{J_1^2(r_n)}\left[F_{1n}(t)+F_{2n}(t)+F_{3n}(t)+F_{4n}(t)-F_{5n}(t)+F_{6n}(t)\right] \quad \dots (50)$$

$$v(r,t)=2\sum_{n=1}^{\infty}\frac{J_0(rr_n)}{J_1^2(r_n)}\left[F_{7n}(t)+F_{8n}(t)+F_{9n}(t)+F_{10n}(t)-F_{11n}(t)+F_{12n}(t)\right] \quad \dots (51)$$

$$\theta(r,t)=2\sum_{n=1}^{\infty}\frac{J_0(rr_n)}{J_1^2(r_n)}F_{13n}(t) \quad \dots (52)$$

$$\phi(r,t)=2\sum_{n=1}^{\infty}\frac{J_0(rr_n)}{J_1^2(r_n)}F_{14n}(t) \quad \dots (53)$$

4.0 Results and Discussions

In this section, we present graphically, the numerical discussion of the results for the velocity field of electro magneto-hydrodynamic of blood flow through a straight tube with an inclined magnetic field. We generated the solutions of the blood velocity, concentration profile and temperature distribution using the MATHCAD code and described the influence of the physical parameters associated with the flow equations. By considering the influence of imposed electric field on both the blood velocity and motion of the magnetic nanoparticles, the effects of the corresponding governing parameters of magnetic field and ratio of zeta potential, fractional order parameter and thermal radiation parameter are presented below:

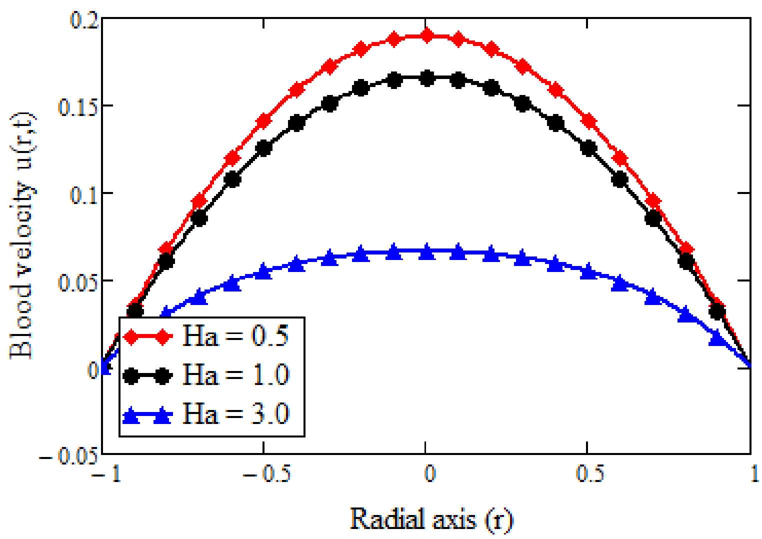

Figure 1: Blood Velocity u(r,t) for Different Values of Magnetic Field Parameter Ha

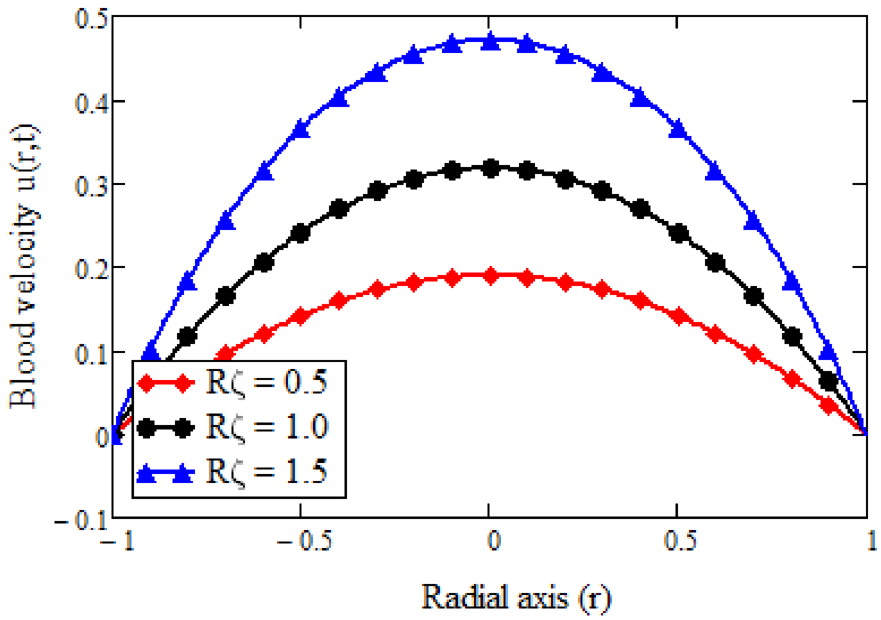

Figure 2: Blood Velocity u(r,t) for Different Values of Zeta Potential Ratio

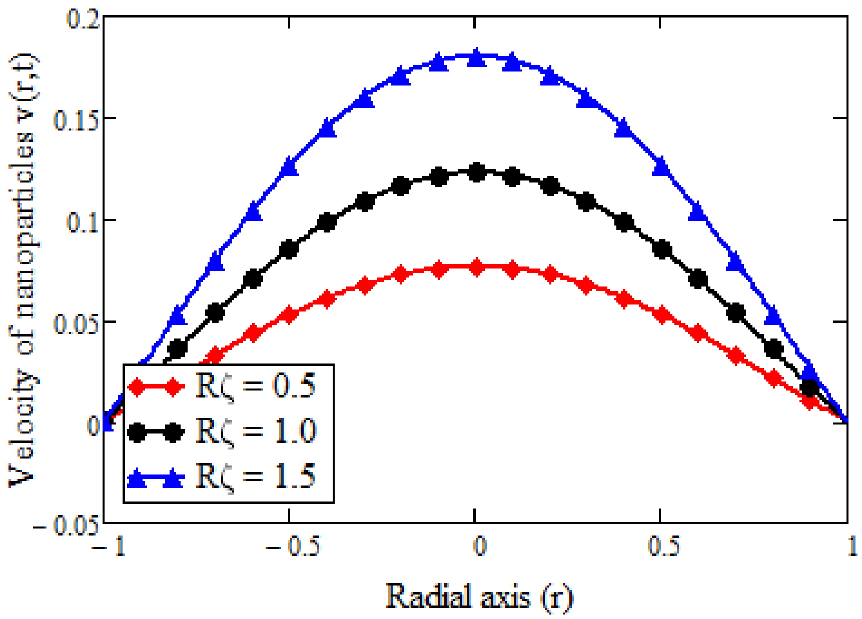

Figure 3: Magnetic nanoparticle Velocity v(r,t) for Different Values of Zeta Potential Ratio

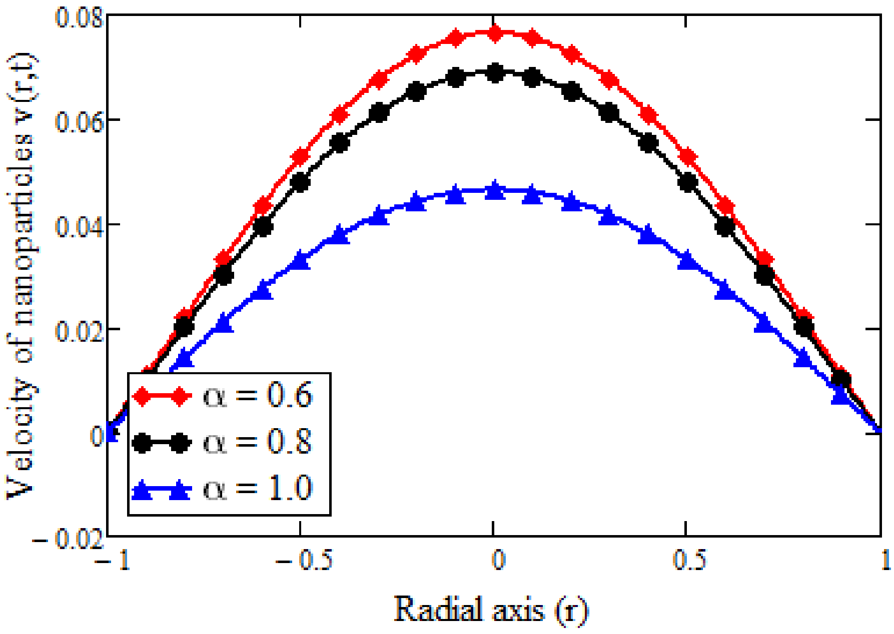

Figure 4: Magnetic nanoparticle Velocity v(r,t) for Different Values of Fractional order parameter α

Figure 1 and shows the effect of magnetic field parameter on the blood velocity, it was observed that increasing intensity of magnetic field parameter decreases both the velocity of the blood and magnetic nanoparticles which slow down the flow rates over the affected region. Hence, for a higher value of magnetic field parameter, the electromagnetic forces were higher, this implies that the electromagnetic forces has a resistive effect on the blood velocity as well as the motion of the magnetic nanoparticles and this occur as a result of the presence of magnetic field which assumed to be electrically conducting parameter and hence lead to the formation of Lorentz force which is responsible for slowing down the motion of blood which leads to the reduction in the velocity profiles of the flow. Also figure 2 and figure 3 show the influence of zeta potential ratio on the velocity of the blood as well as that of magnetic nanoparticles and the figures revealed that increasing the value of zeta potential ratio significantly enhances the velocity of the blood flow from center to neighborhood of arterial wall. It is obvious that when the zeta potential ratio of an applied electric field is high, the repulsive forces out weight the attractive forces, resulting in a relatively stable system and hence provide images of moving drugs to a targeted region.

Figure 4 shows the effect of fractional order parameter α on blood flow velocity It is observed that the both the velocity of the blood and magnetic nanoparticles decreases with increase in the values of the fractional order parameter. This is due to the presence of drug forces on the nanoparticles suspended in the blood. This implies that the fractional order parameter α play a vital role in in controlling the velocity of the blood flow, we note that the velocity of the blood and the velocity of the magnetic nanoparticles are higher for fractional order time derivative than the integer order time derivative. Thus, we conclude that the magnetic drug targeting is more effective for the lower values of α.

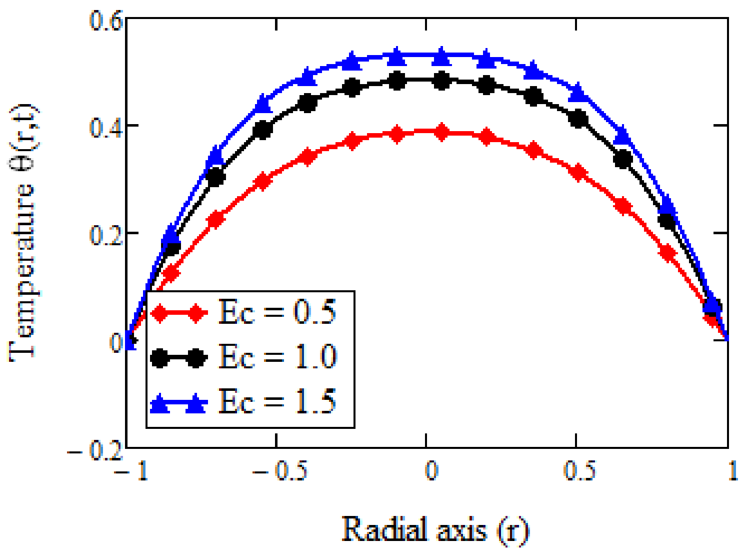

Figure 5; Temperature Distribution for Different Values of Eckert Number Ec

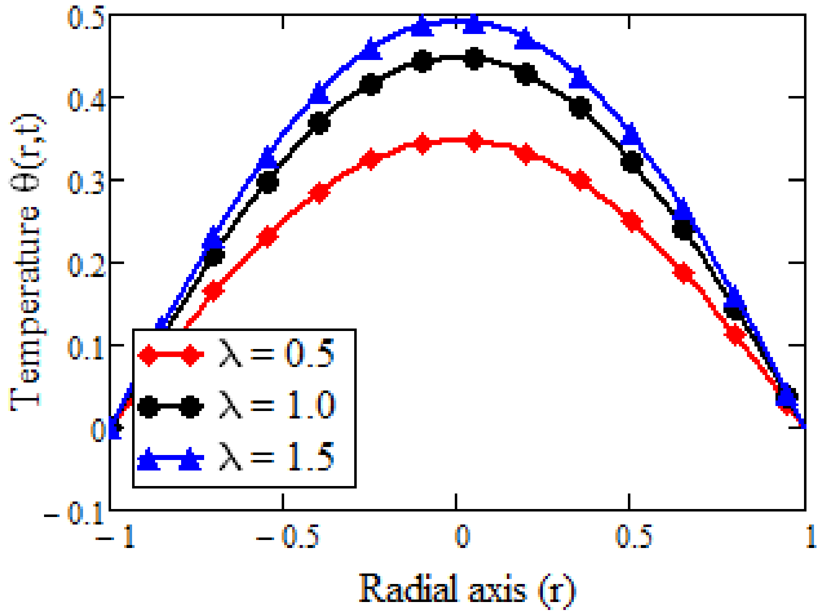

Figure 6: Temperature Distribution for Different Values of Joule Heating Parameter λ

Figures 5 shows the effect of Eckert number on electro-magneto-hydrodynamic blood flow through a straight tube with an inclined magnetic field. It is observed from the figure that when values of Eckert number were varied positively, the temperature increases to a certain level, which implies that the rate of heat transfer was high. This indicates that heat transfer is taking place at the vessel which rises the temperature of the blood. Physically, this implies that as Eckert number increases, the mass transfer dominates the heat dissipation potential which causes the temperature of the blood in the affected region rises to a significant level during tumor treatments. Figures 6 shows the effect of Joule heating parameter on electro-magneto-hydrodynamic blood flow through a straight tube with an inclined magnetic field. It is observed from the figure that the temperature rises rapidly with an increase in the values of joule heating parameter, which implies that heat transfer in the blood flow can be control by adjusting positive values of Joule heating parameter.

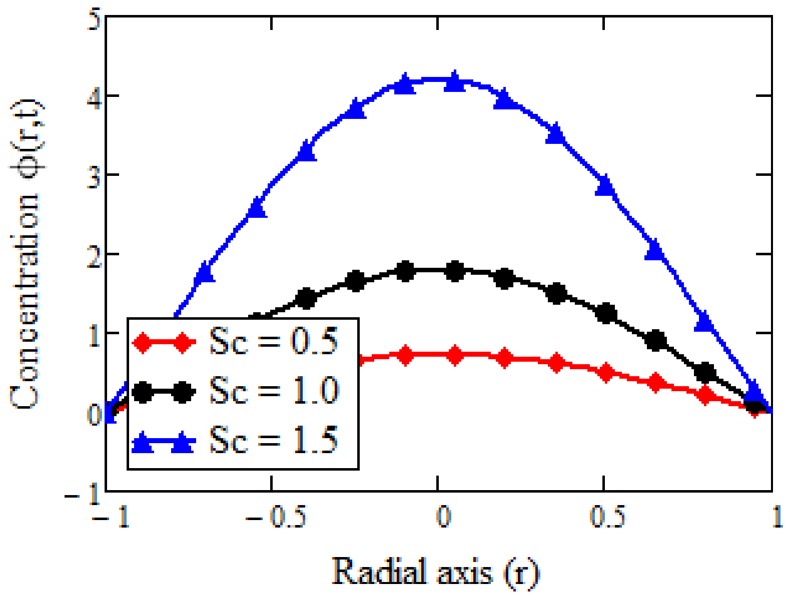

Figure 7: Concentration Profile for Different Values of Schmidt Number Sc

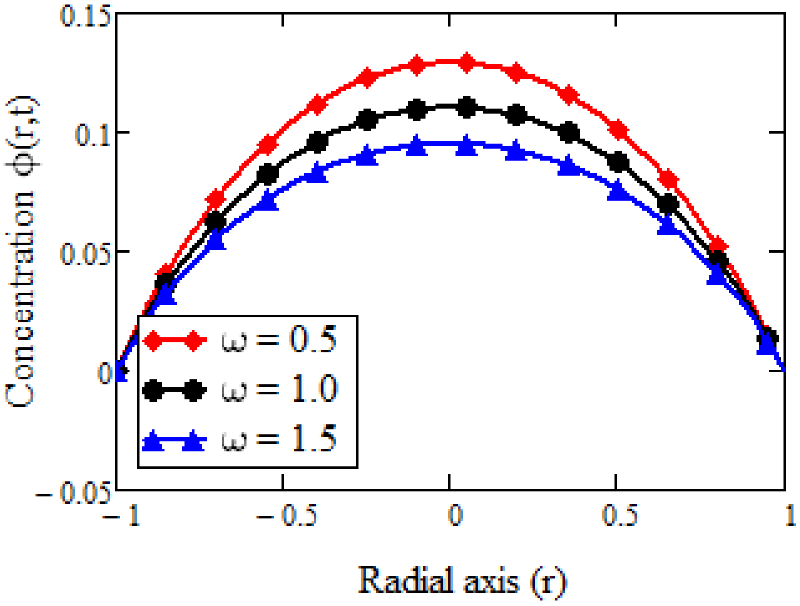

Figure 8: Concentration Profile for Different Values of Chemical reaction parameter

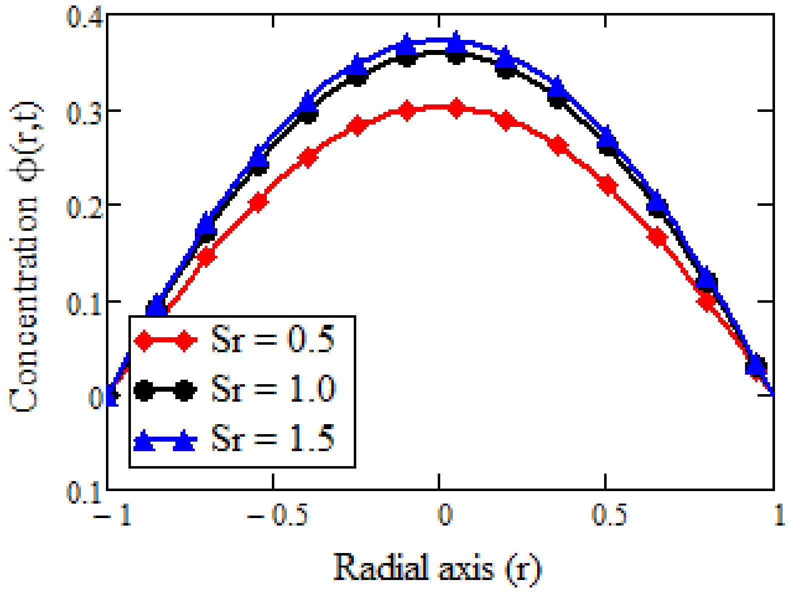

Figure 9: Concentration Profile for Different Values of Soret number Sr

Figures 7, 8 and 9 were plotted to show the effect of Schmidt number, chemical reaction parameter and Soret number on concentration profile in electro-magneto-hydrodynamic blood flow through a straight tube with an inclined magnetic field in tumor treatments by using thermal radiation and chemotherapy. Figure 7, show that the concentration of the blood increases as the value of Schmidt number increases. It was observed from figure 8 that increasing the value of chemical reaction parameter decreases the concentration profile. In the absence of chemical reaction effect, the concentration of the blood becomes higher. The chemical reaction effect of blood concentration would be helpful in various medical therapies such as the Catheter insertion and others. Figure 9 shows the effect of Soret number or thermal-diffusion on the blood concentration, with increase in the values of Soret number the blood concentration increases gradually. This is because the Soret effect or the thermal-diffusion effect produces a concentration flux between lower and higher species concentration, which is driven by the temperature gradient.

4.0 Conclusion

The electrically conducting blood in motion and the effects of an external inclined magnetic field and heat radiation in porous medium vessel for drug delivery applications have been studied in this work. The mathematical formulation for the momentum, concentration and energy equations ware obtained for the blood flow considered to be non-Newtonian. The resulting equations of motion were solved analytically using the method of Laplace transform and finite Hankel transform technique. Various fluid parameters were introduced. The findings of these study clearly revealed that:

I. An increase in the magnetic field and thermal radiation parameter, decreases the velocity of the blood flow due to the presence of the Lorentz force which resist the motion of the blood.

II. Increase in the values of the fractional order parameter, decreases the flow velocity, which means that the fractional order parameter α play a vital role in in controlling the velocity of the blood flow, Thus, we conclude that the magnetic drug targeting is more effective for the lower values of fractional order parameter.

III. Under the influence of an applied electric field, thermal radiation and magnetic field, there is a greater variation of the blood flow in the diverging region than at the converging region.

IV. By increasing the heat radiation parameter, we observed that the curves representing both the velocity and temperature profiles increases rapidly from the origin.

V. Since the study takes into account the effect of an applied electric field and the joule heating effect on blood velocity and temperature respectively, it bears the potential to furnish some additional information regarding the causes and development of arterial diseases, such as atherosclerosis, tumor, blood cancer etc. It is worthwhile to mention here the conjecture made by Chato (1980) and Kumar et.al (2021) that arterial diseases, like atherosclerosis occur mostly in regions, where blood velocity is low.

References:

Akar, S., Esfahani, J. A., & Shaegh, S. A. M. (2019). A numerical investigation of magnetic field

effect on blood flow as biomagnetic fluid in a bend vessel. *Journal of Magnetism and Magnetic Materials*, *482*, 336-349.

Akbarzadeh, P. (2016). The analysis of MHD blood flows through porous arteries using a locally modified homogenous nano-fluids model. *Bio-medical materials and engineering.* 27(1) 15-28.

Ali, F., Sheikh, N. A., Khan, I., & Saqib, M. (2017). Magnetic field effect on blood flow of Casson

fluid in axisymmetric cylindrical tube: A fractional model. *Journal of Magnetism and Magnetic Materials*, *423*, 327-336.

Ellahi R, & Riaz A. (2010), Analytical solutions for MHD flow in a third grade fluid with variable viscosity. *Math Comput Modell*. 52(9), 1783–1793.

Jain M, Sharma GC, Singh R. (2010). Mathematical modelling of blood flow in a stenosed artery under MHD effect through porous medium. *International Journal of Engineering Transactions B: Applications*, 23(3&4):243-251.

Maiti, S., Shaw, S., & Shit, G. C. (2021). Fractional order model for thermochemical flow of blood

with Dufour and Soret effects under magnetic and vibration environment. *Colloids and Surfaces B: Biointerfaces*, *197*, 111395.

Maiti, S., Shaw, S., & Shit, G. C. (2020). Caputo–Fabrizio fractional order model on MHD blood

flow with heat and mass transfer through a porous vessel in the presence of thermal radiation. *Physica A: Statistical Mechanics and its Applications*, *540*, 123149.

Perdikaris, P., & Karniadakis, G. E. (2014). Fractional-order viscoelasticity in one-dimensional blood flow models. *Annals of biomedical engineering*, *42*(5), 1012-1023.

Shah, N. A., & Khan, I. (2016). Heat transfer analysis in a second grade fluid over and oscillating vertical plate using fractional Caputo–Fabrizio derivatives. *The European Physical Journal C*, *76*(7), 1-11.

Shah, N. A., & Khan, I. (2016). Heat transfer analysis in a second grade fluid over and oscillating vertical plate using fractional Caputo–Fabrizio derivatives. *The European Physical Journal C*, *76*(7), 1-11.